

The siRNAsome: A Cation-Free and Versatile Nanostructure for siRNA and Drug Co-delivery

Meng Zheng⁺, Tong Jiang⁺, Wen Yang, Yan Zou, Haigang Wu, Xiuhua Liu, Fengping Zhu, Rongjun Qian, Daishun Ling, Kerrie McDonald, Jinjun Shi, and Bingyang Shi*

Abstract: Nanoparticles show great potential for drug delivery. However, suitable nanostructures capable of loading a range of drugs together with the co-delivery of siRNAs, which avoid the problem of cation-associated cytotoxicity, are lacking. Herein, we report a small interfering RNA (siRNA)-based vesicle (siRNAsome), which consists of a hydrophilic siRNA shell, a thermal- and intracellular-reduction-sensitive hydrophobic median layer, and an empty aqueous interior that meets this need. The siRNAsome can serve as a versatile nanostructure to load drug agents with divergent chemical properties, therapeutic proteins as well as co-delivering immobilized siRNAs without transfection agents. Importantly, the inherent thermal/reduction-responsiveness enables controlled drug loading and release. When siRNAsomes are loaded with the hydrophilic drug doxorubicin hydrochloride and anti-P-glycoprotein siRNA, synergistic therapeutic activity is achieved in multidrug resistant cancer cells and a tumor model.

The use of small interfering RNA (siRNA) to suppress the activity of specific genes is a novel therapeutic option for disease therapy.^[1] However, lack of safe and efficient delivery carriers impedes the development of RNA interference (RNAi) therapeutics for potential clinical use.^[2] The most commonly used siRNA delivery systems are cationic and include polymers,^[3] lipids,^[4] and inorganic materials.^[5] These cationic materials compress siRNAs into nanoformulated polyplexes through electrostatic interaction to enable siRNAs to enter cells and, crucially, avoid nuclease digestion. How-

ever, strongly cationic carriers normally induce severe cytotoxicity in normal tissue by destabilizing cell membranes.^[6] They can also interact with the anionic proteins in the plasma, resulting in unstable siRNA polyplexes and rapid clearance.^[7] As such, a new strategy for the development of cation-free siRNA delivery systems is greatly needed. Recently, various nucleic acid nanostructures (NANs), such as spherical nucleic acids (SNAs),^[8] DNA nanoparticles,^[9] and nucleic acid nanogels^[10] have been developed for siRNA delivery, obviating the need for cationic components. These cation-free NANs are incapable of triggering positive-charge-induced cytotoxicity and plasma protein interaction, and thus represent a promising new direction for the construction of carriers for siRNA delivery.

Given the complicated pathological mechanism/s of refractory disease, co-delivery of siRNA in conjunction with other drug types may offer complimentary and more potent efficacy, relative to conventional monotherapeutic strategies.^[11] However, most siRNA and drug co-delivery systems still utilize a cationic component to encapsulate siRNA and are hence subject to the same cytotoxicity potential. Recently, drug-cored^[12] or drug-loaded^[13] micellar SNAs, in which drugs are anchored or encapsulated inside a polymer core together with a nucleic-acid-immobilizing shell, represent a promising approach for siRNA and drug co-delivery without cationic materials. Despite these improvements, these micellar SNAs nanostructures still have a key limitation; the hydrophobic micellar core only allows loading of hydrophobic small

[*] Dr. M. Zheng,^[†] T. Jiang,^[†] W. Yang, Dr. Y. Zou, Dr. H. Wu, Prof. B. Shi Henan and Macquarie University Joint Centre for Biomedical Innovation, School of Life Sciences, Henan University Kaifeng, Henan, 475004 (China)
E-mail: bs@henu.edu.cn

Dr. Y. Zou, Prof. B. Shi
Department of Biomedical Sciences, Faculty of Medicine & Health Sciences, Macquarie University, Sydney, NSW (Australia)

Prof. X. Liu
College of Chemistry and Chemical Engineering, Henan University, Kaifeng, 475004 (China)

Dr. F. Zhu
Department of Neurosurgery, Huashan Hospital, Fudan University, Shanghai, 200040, (China)

Dr. R. Qian
Department of Neurosurgery, The Henan Provincial People's Hospital, Zhengzhou, 450003 (China)

Prof. D. Ling
Zhejiang Province Key Laboratory of Anti-Cancer Drug Research, College of Pharmaceutical Sciences, Zhejiang University, Hangzhou, 310058 (China)

Prof. K. McDonald
Cure Brain Cancer Foundation Biomarkers and Translational Research Group, Prince of Wales Clinical School, Lowy Cancer Research Centre, University of New South Wales, Sydney, NSW (Australia)

Prof. J. Shi, Prof. B. Shi
Center for Nanomedicine and Department of Anesthesiology, Brigham and Women's Hospital, Harvard Medical School, Boston, MA (USA)

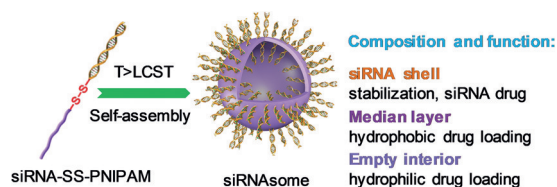
[†] These authors contributed equally to this work.

Supporting information and the ORCID identification number(s) for the author(s) of this article can be found under: <https://doi.org/10.1002/anie.201814289>.

© 2019 The Authors. Published by Wiley-VCH Verlag GmbH & Co. KGaA. This is an open access article under the terms of the Creative Commons Attribution Non-Commercial NoDerivs License, which permits use and distribution in any medium, provided the original work is properly cited, the use is non-commercial, and no modifications or adaptations are made.

molecules,^[14] excluding a myriad of hydrophilic molecules and proteins. Consequently, developing a cation-free versatile nanostructure, also capable of loading hydrophilic small drugs and biomolecular payloads, is highly desirable.

Here, we constructed a novel drug delivery nanostructure, an siRNA-based vesicle (siRNAsome), originating from the self-assembly of siRNA-disulfide-poly(*N*-isopropylacrylamide) (siRNA-SS-PNIPAM) diblock copolymers (Scheme 1). The resultant siRNAsome consists of a hydro-



Scheme 1. Illustration of siRNAsome formation, composition, and function. T > LCST = Temperature greater than the lower critical solution temperature.

philic siRNA stabilization shell, a temperature- and intracellular-reduction-sensitive hydrophobic median layer, and an empty aqueous interior. This design enables hydrophilic small molecules and biomolecules to be encapsulated within the vesicular interior as the polymersome is fabricated,^[15] but critically, also enables hydrophobic small molecules or drugs to be incorporated into a temperature-responsive hydrophobic layer. Thus, the siRNAsome technology can co-deliver immobilized siRNAs plus loaded small-molecule drugs or proteins into cells without using cationic agents. To our knowledge, this is the first report of an siRNAsome and its promising potential in drug co-delivery.

siRNA-SS-PNIPAM was readily prepared by an exchange reaction between PNIPAM orthopyridyl disulfide (PNIPAM-SS-Py) and mercapto siRNA (siRNA-SH). The synthetic approach is illustrated in Figure S1 in the Supporting Information. Firstly, PNIPAM (characterization data is presented in Table S1 in the Supporting Information) terminated with a carboxyl group was reacted with 2-(2-pyridyldithio)ethylamine to yield PNIPAM-SS-Py. The ¹H NMR data showed that the conversion ratio of carboxyl groups to -SS-Py groups was 90% (Supporting Information, Figure S2). After 24 h, the resulting polymer from the exchange reaction between PNIPAM-SS-Py and siRNA-SH, was purified by dialysis, centrifugation, and washed with isopropanol to remove byproducts, unreacted siRNA and PNIPAM. Ultra performance liquid chromatography (UPLC) results show that the resulting siRNA-SS-PNIPAM copolymer was narrowly dispersed with a single peak, free from unreacted siRNA and PNIPAM (Supporting Information, Figure S3), thereby indicating the successful synthesis and purification of siRNA-SS-PNIPAM.

As PNIPAM is temperature-responsive,^[16] siRNA-SS-PNIPAM copolymers can self-assemble into nanoparticles upon heating, with a lower critical solution temperature (LCST) of 30 °C, 31 °C, and 32 °C for PNIPAM components of 7 kDa, 13 kDa, and 19 kDa, respectively (Supporting Information, Table S2). This enables nanoparticles to control drug

loading during the self-assembly process. Gel retardation assays show that after siRNA-SS-PNIPAM heating, no free siRNA was released and all siRNA stayed in the initial position (Figure 1a), further confirming successful nanopar-

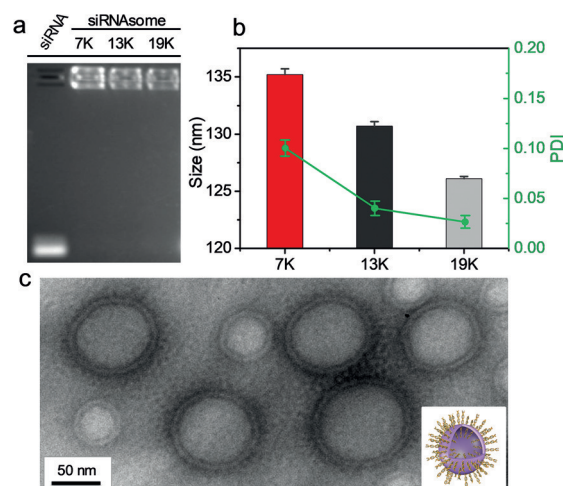


Figure 1. Characterization of the siRNAsome. a) Gel electrophoresis and b) size and polydispersity index (PDI) of siRNAsomes derived from PNIPAMs of different molecular weights; c) TEM image of siRNAsomes derived from PNIPAMs of 19 kDa in molecular weight.

ticle formulation. Dynamic light scattering (DLS) measurements show that the formulated nanoparticles ranged in particle size from 126 nm to 135 nm (Figure 1b and Supporting Information, Table S2) while exhibiting very narrow polydispersity index (PDI). Transmission electron microscopy (TEM) images further confirmed the particle size. More importantly, a clear vesicular morphology, with an empty interior and a solid layer, was observed in nanoparticles derived from PNIPAMs of three different molecular weights (Figure 1c and Supporting Information, Figure S4), indicating the successful formation of siRNAsome. Furthermore, the siRNAsomes are very stable under physiological condition, their particle size was constant and no siRNA release was observed even after up to 7 days of storage (Supporting Information, Figure S5). The siRNAsomes derived from PNIPAMs of 19 kDa in molecular weight showed the best dilution stability (lowest critical aggregation concentration, CAC; Supporting Information, Table S2). Using PNIPAM of this molecular weight, the drug-loading utility of siRNAsome was confirmed by performing an encapsulation experiment using the hydrophilic drug doxorubicin hydrochloride (Dox-HCl), the hydrophobic drug docetaxel (DTX), and the hydrophilic protein bovine serum albumin (BSA). As shown in Tables S3 in the Supporting Information, successful encapsulation of Dox-HCl, DTX, and BSA was achieved during the siRNAsome fabrication process. Using siRNA-SS-PNIPAM copolymer, upon heating, loading efficacies of approximately 37%, 43%, and 33% (for Dox-HCl, DTX, and BSA, respectively) were achieved at a theoretical drug loading content of 20 wt.%. These data confirm that the siRNAsome

nanostructure can serve as a uniquely versatile carrier for therapeutic agents with diverse chemical properties and types.

To ensure siRNAsomes could lead to intracellular-environment-triggered drug release in cells, a redox-sensitive disulfide bond,^[17] covalently linking the siRNA and PNIPAM, was incorporated into the siRNAsome. To confirm whether intracellular redox conditions can rupture this bond, leading to cargo release, siRNAsome nanoparticles were treated with 10 mM dithiothreitol (DTT) solution at 37°C for different durations (0–24 h) and assessed by gel electrophoresis and DLS/TEM measurements. As shown in Figure 2 a, gel electro-

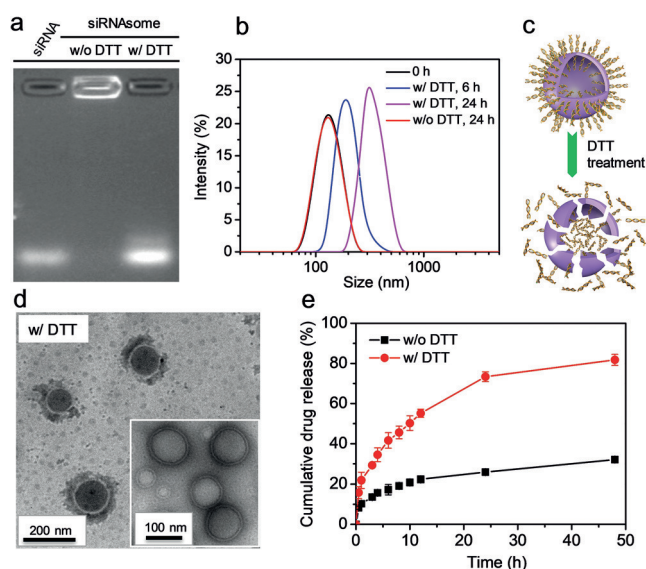


Figure 2. Responsiveness of siRNAsomes to a reducing environment. a) siRNA release determined by gel electrophoresis. b) Modulation of nanoparticle size determined by DLS. c) Schematic representation of siRNAsome disruption and d) siRNAsome structure disruption assessed by TEM imaging (inset is unreduced siRNAsome structure). e) Dox-HCl release from siRNAsome over time.

phoresis clearly showed siRNA release, supporting our hypothesis that the introduced disulfide bond was vulnerable to reducing cellular environments, triggering the cleavage of siRNA–SS–PNIPAM. DLS measurements showed that siRNAsomes maintained essentially the same particle size (126 nm) after 24 h in the absence of DTT, indicating excellent colloidal stability of the siRNA shell-stabilized nanoparticles. However, the siRNAsomes rapidly expanded to approximately 235 nm and 341 nm in size following 6 h and 24 h incubation with 10 mM DTT (Figure 2b), respectively, indicating that reduction results in siRNAsome swelling. Cleavage of the disulfide bond and destruction of the vesicle structure is illustrated in Figure 2c and further confirmed by TEM. As shown in Figure 2d, the vesicle structure was disrupted after 12 h incubation with 10 mM DTT. The interior of the siRNAsomes became black due to the staining of released siRNA, while the unreduced siRNAsomes possessed a clear-colored interior (Figure 2d). This suggests that reduction triggers disulfide cleavage and siRNA release. The kinetics of drug release were then monitored. As shown in Figure 2e, the siRNAsomes released Dox-HCl rapidly in

the presence of 10 mM DTT. After 24 h treatment with DTT, more than 75 % of the encapsulated drugs were released. In contrast, less drug release, 23 %, was observed after 24 h without DTT treatment. Drug release was gradual, with a constant release rate, indicating the potential for a better drug exposure profile.

To confirm the ability of siRNAsomes to deliver siRNAs into cells, without the assistance of any cationic agents, multidrug resistant (MDR) MCF-7 cells were incubated with FAM-labeled siRNAsomes. As shown in Figure 3 a, siRNA-

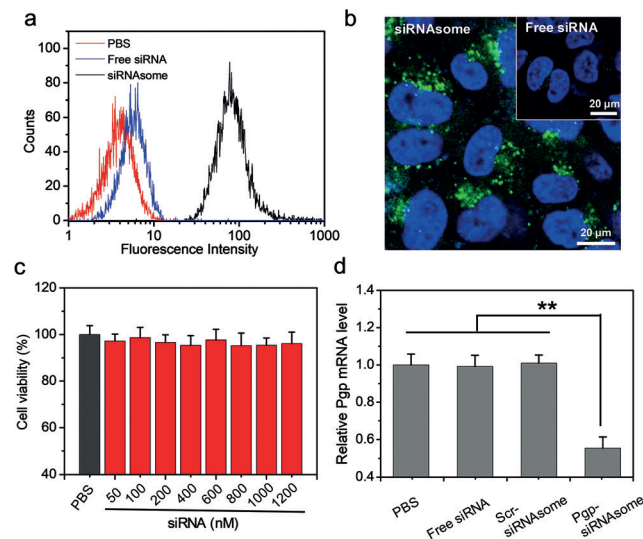


Figure 3. In vitro performance of siRNAsomes in MDR MCF-7 cells. a) Flow cytometry and b) confocal microscopy assays show cellular uptake of siRNAsomes. In both experiments, siRNAs were labeled with FAM dye. c) Cell viability assay of MDR MCF-7 cells incubated with siRNAsomes (siRNA concentration ranging from 50 to 1200 nM) shows good biocompatibility and safety. d) Gene silencing of Pgp mRNA level as determined by RT-PCR assay.

somes were efficiently taken up by cells, compared to free siRNA. The enhanced cellular uptake of siRNAsomes was further confirmed by confocal laser scanning microscopy (CLSM) imaging (Figure 3b). The efficient cellular uptake ability of the siRNAsomes could be mediated by endocytosis after binding to class A scavenger receptors.^[8a,18] Interestingly, the high uptake of siRNAsomes in MDR MCF-7 cells did not cause any measurable toxicity, even at a high siRNA concentration of 1200 nM (Figure 3c), indicating the excellent biocompatibility of the cation-free siRNAsome. Previous studies have highlighted the role played by the P-glycoprotein (Pgp) in the development of drug resistance,^[19] as Pgp effectively pumps out administered drugs. To determine whether the siRNAsomes could effectively deliver Pgp-gene-silencing siRNAs into MDR MCF-7 cells, MCF-7 MDR cells were incubated with siRNAsomes incorporating Pgp-siRNA for 2 days and then Pgp mRNA expression was detected using real-time (RT) PCR. After sequence-specific Pgp gene silencing by the siRNAsome, the Pgp mRNA expression level was reduced by approximately 42 %, at an siRNA concentration of 200 nM (Figure 3d). This study indicates the cation-free siRNAsomes can deliver attached

Pgp-siRNA to target the Pgp drug exporter, and shows its potential to overcome drug resistance of MDR cells. Thus, siRNAsomes attached to Pgp-siRNA, combined with anti-cancer drugs, may offer enhanced MDR cell killing by inducing synergistic therapeutic effects.

Pgp-siRNA and Dox-HCl were co-delivered to test the synergistic potential of the siRNAsomes against MDR cancer cells (Figure 4a). Flow cytometry, confocal imaging, and the MTT assay were used to evaluate cytotoxicity and efficacy. Cytotoxicity assessments demonstrated that Pgp mRNA knockdown significantly improved the activity of Dox-HCl, whereas scrambled (control) siRNAs and free Dox-HCl had much lower effect (Figure 4b). Furthermore, in non-MDR i.e., MCF-7, cells, which do not actively pump out Dox-HCl, the siRNAsomes (Dox-HCl loaded) attached with scrambled siRNAs or Pgp-siRNAs had similar cytotoxicity, which was lower than that of Dox-HCl under the same conditions (Supporting Information, Figure S6a). These results suggest the synergistic effect of Pgp-siRNA and Dox-HCl against MDR cells. In contrast, Dox-HCl administration without Pgp mRNA knockdown or siRNAsome-based delivery, resulted in less cytotoxicity as the MDR cells could efflux Dox-HCl. These data were corroborated by the increased fluorescence intensity of Dox-HCl in cells receiving co-delivered Pgp-siRNA compared to cells treated with free drug or nanoparticles delivering Dox-HCl with scrambled siRNA (Fig-

ure 4c). These data are further confirmed by CLSM that shows more Dox-HCl (red fluorescence) present inside MDR MCF-7 cells when treated with siRNAsomes attached to Pgp-siRNA (Supporting Information, Figure S7). It should also be noted that treatment of non-MDR MCF-7 cells with siRNAsomes (Dox-HCl loaded) attached to scrambled siRNAs or Pgp-siRNAs resulted in similar Dox-HCl fluorescence intensities. This level of fluorescence intensity was reduced in comparison to non-MDR MCF-7 cells treated with free Dox-HCl under the same conditions (Supporting Information, Figure S6b,c). Furthermore, the in vivo delivery ability of the siRNAsome was evaluated. As shown in Figure S8 in the Supporting Information, more Dox-HCl accumulated in the tumor when using siRNAsome-based delivery in comparison with treatment with free Dox-HCl. Subsequently, the tumor growth inhibition ability of the siRNAsome was tested in an MDR MCF-7 subcutaneous tumor model by co-delivering Dox-HCl and Pgp-siRNA. Impressively, the Dox-HCl-loaded siRNAsomes attached to Pgp-siRNA displayed the strongest tumor growth inhibition ability (Figure 4d), which is in line with the in vitro performance, with negligible body weight changes (Figure 4e). Collectively, these results show that the siRNAsome can co-deliver Dox-HCl and Pgp-siRNA to achieve synergistic therapeutic efficacy against MDR cancer cells and a tumor model.

In summary, we have fabricated a unique siRNA-based vesicle, termed the siRNAsome. This can serve as a versatile nanostructure to deliver payloads of small-molecule drugs and biomolecular agents that have divergent chemical properties. Importantly, by exploiting the temperature- and intracellular-reduction-responsiveness, drug loading into the siRNAsome and drug release in cells can be controlled. Moreover, incorporation of a siRNA shell not only stabilizes the nanoparticle, but provides the opportunity to deliver drug-action-complementary siRNAs, thus realizing siRNA co-delivery with other drug types. The utility of this design was demonstrated by showing that the siRNAsomes attached to Pgp-siRNA and loaded with Dox-HCl displayed improved synergistic efficacy against MDR MCF-7 cancer both in vitro and in vivo. We expect that our cation-free siRNAsome could serve as a versatile nanostructure for drug, therapeutic protein, and siRNA co-delivery to target a broad range of diseases.

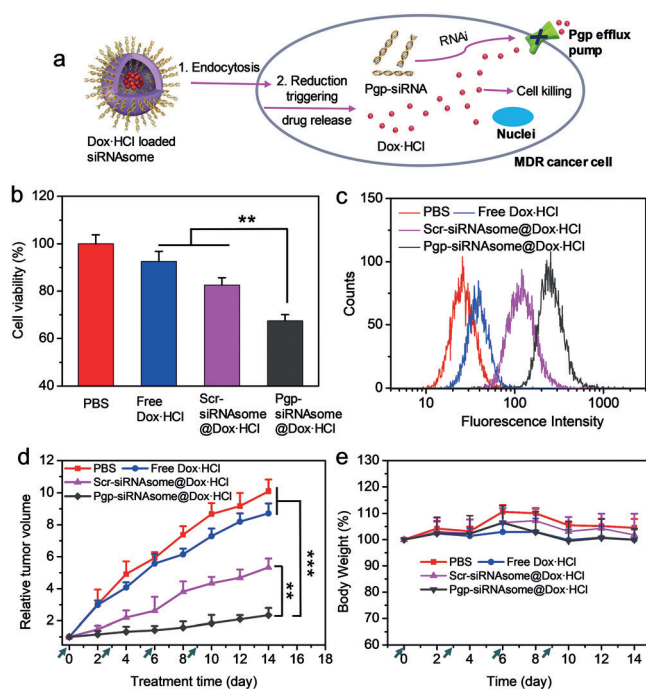


Figure 4. Synergistic therapy against MDR MCF-7 cancer cells and tumor model by using siRNAsomes to co-deliver Dox-HCl and Pgp-siRNA. a) Schematic representation of the synergistic mechanism of the co-delivery of Dox-HCl and Pgp-siRNA by the siRNAsome into MDR cancer cells. b) Cell viability of MDR MCF-7 cells treated with Dox-HCl-loaded siRNAsomes and controls. c) Dox-HCl fluorescence intensity in MDR MCF-7 cells, determined by flow cytometry. d) Tumor growth profiles of MDR MCF-7 tumor-bearing mice treated with Dox-HCl-loaded siRNAsomes and its controls. e) Relative body weights of the mice during the tumor-growth inhibition study.

Acknowledgements

This work was supported by the National Natural Science Foundation of China (NSFC 31600809, 31800841, U1604177, and U1804139), the National Key Technologies R&D Program of China (2018YFA0209800), the Program of China's 1000-Talents Plan, the Key Research Program in Colleges and Universities of Henan Province (19zx006), the Australian Endeavour Fellowship (No.69172018), the Mason Foundation National Medical Program (MAS2017F034), and the National Health and Medical Research Council (NHMRC) Dementia Fellowship (APP1111611).

Conflict of interest

The authors declare no conflict of interest.

Keywords: co-delivery · nanostructures · siRNA · synergistic therapy · vesicles

How to cite: *Angew. Chem. Int. Ed.* **2019**, *58*, 4938–4942
Angew. Chem. **2019**, *131*, 4992–4996

- [1] a) A. Reynolds, D. Leake, Q. Boese, S. Scaringe, W. S. Marshall, A. Khvorova, *Nat. Biotechnol.* **2004**, *22*, 326–330; b) M. L. Bobbin, J. J. Rossi, *Annu. Rev. Pharmacol. Toxicol.* **2016**, *56*, 103–122; c) A. Wittrup, A. Ai, X. Liu, P. Hamar, R. Trifonova, K. Charisse, M. Manoharan, T. Kirchhausen, J. Lieberman, *Nat. Biotechnol.* **2015**, *33*, 870–876.
- [2] a) J. M. Wells, L. H. Li, A. Sen, G. P. Jahreis, S. W. Hui, *Gene Ther.* **2000**, *7*, 541–547; b) K. A. Whitehead, R. Langer, D. G. Anderson, *Nat. Rev. Drug Discovery* **2009**, *8*, 129–138; c) M. Zheng, W. Tao, Y. Zou, O. C. Farokhzad, B. Shi, *Trends Biotechnol.* **2018**, *36*, 562–575.
- [3] a) T. Yu, X. Liu, A. L. Bolcato-Bellemin, Y. Wang, C. Liu, P. Erbacher, F. Ou, P. Rocchi, J. P. Behr, L. Peng, *Angew. Chem. Int. Ed.* **2012**, *51*, 8478–8484; *Angew. Chem.* **2012**, *124*, 8606–8612; b) C. Y. Sun, S. Shen, C. F. Xu, H. J. Li, Y. Liu, Z. T. Cao, X. Z. Yang, J. X. Xia, J. Wang, *J. Am. Chem. Soc.* **2015**, *137*, 15217–15224; c) Y. Zou, M. Zheng, W. J. Yang, F. H. Meng, K. Miyata, H. J. Kim, K. Kataoka, Z. Y. Zhong, *Adv. Mater.* **2017**, *29*, 1703285.
- [4] a) K. Buyens, S. C. De Smedt, K. Braeckmans, J. Demeester, L. Peeters, L. A. van Grunsvan, X. de Mollerat du Jeu, R. Sawant, V. Torchilin, K. Farkasova, M. Ogris, N. N. Sanders, *J. Controlled Release* **2012**, *158*, 362–370; b) M. Jayaraman, S. M. Ansell, B. L. Mui, Y. K. Tam, J. Chen, X. Du, D. Butler, L. Eltepu, S. Matsuda, J. K. Narayanannair, K. G. Rajeev, I. M. Hafez, A. Akinc, M. A. Maier, M. A. Tracy, P. R. Cullis, T. D. Madden, M. Manoharan, M. J. Hope, *Angew. Chem. Int. Ed.* **2012**, *51*, 8529–8533; *Angew. Chem.* **2012**, *124*, 8657–8661; c) O. S. Fenton, K. J. Kauffman, R. L. McClellan, J. C. Kaczmarek, M. H. D. Zeng, J. L. Andresen, L. H. Rhym, M. W. Heartlein, F. DeRosa, D. G. Anderson, *Angew. Chem. Int. Ed.* **2018**, *57*, 13582–13586; *Angew. Chem.* **2018**, *130*, 13770–13774.
- [5] a) J. Conde, A. Ambrosone, Y. Hernandez, F. R. Tian, M. McCully, C. C. Berry, P. V. Baptista, C. Tortiglione, J. M. de la Fuente, *Nano Today* **2015**, *10*, 421–450; b) V. Sokolova, M. Epple, *Angew. Chem. Int. Ed.* **2008**, *47*, 1382–1395; *Angew. Chem.* **2008**, *120*, 1402–1416; c) Y. L. Liu, X. Y. Ji, W. W. L. Tong, D. Askhatova, T. Y. Yang, H. W. Cheng, Y. Z. Wang, J. J. Shi, *Angew. Chem. Int. Ed.* **2018**, *57*, 1510–1513; *Angew. Chem.* **2018**, *130*, 1526–1529.
- [6] a) J. H. Kuo, M. S. Jan, H. W. Chiu, *J. Pharm. Pharmacol.* **2005**, *57*, 489–495; b) S. M. Moghimi, P. Symonds, J. C. Murray, A. C. Hunter, G. Debska, A. Szewczyk, *Mol. Ther.* **2005**, *11*, 990–995; c) A. C. Hunter, *Adv. Drug Delivery Rev.* **2006**, *58*, 1523–1531; d) Y. J. Choi, S. J. Kang, Y. J. Kim, Y. B. Lim, H. W. Chung, *Drug Chem. Toxicol.* **2010**, *33*, 357–366.
- [7] B. Ballarín-González, K. A. Howard, *Adv. Drug Delivery Rev.* **2012**, *64*, 1717–1729.
- [8] a) J. I. Cutler, E. Auyeung, C. A. Mirkin, *J. Am. Chem. Soc.* **2012**, *134*, 1376–1391; b) S. A. Jensen, E. S. Day, C. H. Ko, L. A. Hurley, J. P. Luciano, F. M. Kouri, T. J. Merkel, A. J. Luthi, P. C. Patel, J. I. Cutler, W. L. Daniel, A. W. Scott, M. W. Rotz, T. J. Meade, D. A. Giljohann, C. A. Mirkin, A. H. Stegh, *Sci. Transl. Med.* **2013**, *5*, 209ra152; c) R. J. Banga, N. Chernyak, S. P. Narayan, S. T. Nguyen, C. A. Mirkin, *J. Am. Chem. Soc.* **2014**, *136*, 9866–9869; d) W. M. Ruan, M. Zheng, Y. An, Y. Y. Liu, D. B. Lovejoy, M. C. Hao, Y. Zou, A. Lee, S. Yang, Y. Q. Lu, M. Morsch, R. Chung, B. Y. Shi, *Chem. Commun.* **2018**, *54*, 3609–3612.
- [9] a) H. Lee, A. K. R. Lytton-Jean, Y. Chen, K. T. Love, A. I. Park, E. D. Karagiannis, A. Sehgal, W. Querbes, C. S. Zurenko, M. Jayaraman, C. G. Peng, K. Charisse, A. Borodovsky, M. Manoharan, J. S. Donahoe, J. Truelove, M. Nahrendorf, R. Langer, D. G. Anderson, *Nat. Nanotechnol.* **2012**, *7*, 389–393; b) M. A. Rahman, P. F. Wang, Z. X. Zhao, D. S. Wang, S. Nannapaneni, C. Zhang, Z. J. Chen, C. C. Griffith, S. J. Hurwitz, Z. G. Chen, Y. G. Ke, D. M. Shin, *Angew. Chem. Int. Ed.* **2017**, *56*, 16023–16027; *Angew. Chem.* **2017**, *129*, 16239–16243.
- [10] F. Ding, Q. B. Mou, Y. Ma, G. F. Pan, Y. Y. Guo, G. S. Tong, C. H. J. Choi, X. Y. Zhu, C. Zhang, *Angew. Chem. Int. Ed.* **2018**, *57*, 3064–3068; *Angew. Chem.* **2018**, *130*, 3118–3122.
- [11] a) C. Chu, E. Ren, Y. Zhang, J. Yu, H. Lin, X. Pang, Y. Zhang, H. Liu, Z. Qin, Y. Cheng, X. Wang, W. Li, X. Kong, X. Chen, G. Liu, *Angew. Chem. Int. Ed.* **2019**, *58*, 269–272; *Angew. Chem.* **2019**, *131*, 275–278; b) Z. J. Deng, S. W. Morton, E. Ben-Akiva, E. C. Dreaden, K. E. Shopsowitz, P. T. Hammond, *ACS Nano* **2013**, *7*, 9571–9584; c) H. Meng, W. X. Mai, H. Y. Zhang, M. Xue, T. Xia, S. J. Lin, X. Wang, Y. Zhao, Z. X. Ji, J. I. Zink, A. E. Nel, *ACS Nano* **2013**, *7*, 994–1005; d) X. Y. Xu, K. Xie, X. Q. Zhang, E. M. Pridgen, G. Y. Park, D. S. Cui, J. J. Shi, J. Wu, P. W. Kantoff, S. J. Lippard, R. Langer, G. C. Walker, O. C. Farokhzad, *Proc. Natl. Acad. Sci. USA* **2013**, *110*, 18638–18643; e) Y. C. Chang, K. Yang, P. Wei, S. S. Huang, Y. X. Pei, W. Zhao, Z. C. Pei, *Angew. Chem. Int. Ed.* **2014**, *53*, 13126–13130; *Angew. Chem.* **2014**, *126*, 13342–13346.
- [12] a) X. Y. Tan, X. G. Lu, F. Jia, X. F. Liu, Y. H. Sun, J. K. Logan, K. Zhang, *J. Am. Chem. Soc.* **2016**, *138*, 10834–10837; b) X. Y. Tan, B. B. Li, X. G. Lu, F. Jia, C. Santori, P. Menon, H. Li, B. H. Zhang, J. J. Zhao, K. Zhang, *J. Am. Chem. Soc.* **2015**, *137*, 6112–6115.
- [13] S. S. Zhu, H. Xing, P. Gordichuk, J. Park, C. A. Mirkin, *Adv. Mater.* **2018**, *30*, 1707113.
- [14] a) K. Kataoka, A. Harada, Y. Nagasaki, *Adv. Drug Delivery Rev.* **2012**, *64*, 37–48; b) H. Cabral, K. Kataoka, *J. Controlled Release* **2014**, *190*, 465–476.
- [15] a) V. Balasubramanian, B. Herranz-Blanco, P. V. Almeida, J. Hirvonen, H. A. Santos, *Prog. Polym. Sci.* **2016**, *60*, 51–85; b) J. S. Lee, J. Feijen, *J. Controlled Release* **2012**, *161*, 473–483; c) F. H. Meng, Z. Y. Zhong, *J. Phys. Chem. Lett.* **2011**, *2*, 1533–1539.
- [16] A. Halperin, M. Kroger, F. M. Winnik, *Angew. Chem. Int. Ed.* **2015**, *54*, 15342–15367; *Angew. Chem.* **2015**, *127*, 15558–15586.
- [17] a) R. Cheng, F. Feng, F. H. Meng, C. Deng, J. Feijen, Z. Y. Zhong, *J. Controlled Release* **2011**, *152*, 2–12; b) H. Sun, Y. F. Zhang, Z. Y. Zhong, *Adv. Drug Delivery Rev.* **2018**, *132*, 16–32.
- [18] J. I. Cutler, K. Zhang, D. Zheng, E. Auyeung, A. E. Prigodich, C. A. Mirkin, *J. Am. Chem. Soc.* **2011**, *133*, 9254–9257.
- [19] a) G. Housman, S. Byler, S. Heerboth, K. Lapinska, M. Longacre, N. Snyder, S. Sarkar, *Cancers* **2014**, *6*, 1769–1792; b) J. Liu, L. Song, S. Liu, S. Zhao, Q. Jiang, B. Ding, *Angew. Chem. Int. Ed.* **2018**, *57*, 15486–15490; *Angew. Chem.* **2018**, *130*, 15712–15716; c) H. A. Meng, M. Liong, T. A. Xia, Z. X. Li, Z. X. Ji, J. I. Zink, A. E. Nel, *ACS Nano* **2010**, *4*, 4539–4550; d) J. Li, Y. Wang, Y. Zhu, D. Oupicky, *J. Controlled Release* **2013**, *172*, 589–600.

Manuscript received: December 16, 2018

Revised manuscript received: January 23, 2019

Accepted manuscript online: February 9, 2019

Version of record online: March 3, 2019